PROCEEDINGS OF SCIENCE

Measurement of integrated flux of cosmic ray muons at sea level using the India-based Neutrino Observatory prototype detector

Sumanta Pal*
Tata Institute of Fundamental Research, Mumbai 400005, India
E-mail: sumanta@tifr.res.in

G.Majumder
Tata Institute of Fundamental Research, Mumbai 400005, India
E-mail: gobinda@tifr.res.in

N.K.Mondal
Tata Institute of Fundamental Research, Mumbai 400005, India
E-mail: nkm@tifr.res.in

D.Samuel
Tata Institute of Fundamental Research, Mumbai 400005, India
E-mail: samuel@tifr.res.in

B.Satyanarayana
Tata Institute of Fundamental Research, Mumbai 400005, India
E-mail: bsn@tifr.res.in

The India-based Neutrino Observatory (INO) collaboration is planning to set up a magnetized Iron-CALorimeter (ICAL) to study atmospheric neutrino oscillations with precise measurements of oscillations parameters. ICAL uses 50 kton iron as target mass and about 28,800 Resistive Plate Chambers (RPC) of 2 m $\times$ 2 m in area as active detector elements. As part of its R&D program, a prototype detector stack comprising of 12 layers of RPCs of 1 m $\times$ 1 m in area has been set up at Tata Institute of Fundamental Research (TIFR) to study the detector parameters using cosmic ray muons. We present here a study of cosmic ray muon flux measurement at sea level and lower latitude ($18^{\circ}54^{'}$N).

XI workshop on Resistive Plate Chambers and Related Detectors - RCP2012,
February 5-10, 2012
INFN Laboratori Nazionali di Frascati Italy

*Speaker.

PoS(RPC2012)021

1. Introduction

The INO-ICAL is a proposed neutrino physics experiment in India which aims to measure neutrino oscillation parameters and to conduct other studies in neutrino physics. A detailed description of the INO project can be found in the project report [1]. RPCs will be used as active detectors in ICAL to detect charged particles produced by the interaction of neutrinos in the Iron plates. During the R&D program, we have successfully built 3 prototype stacks to study the stability of the detector and other parameters using cosmic ray muons ([2]-[4]). The results presented here are from one of the prototypes at TIFR. Recently, an initiative is taken to harness the full potential of these prototypes by using them for particle physics studies, one of which is to study the flux of cosmic ray muons at sea level. The motivation of this study is to better understand various efficiencies (viz. trigger, tracking) of RPC layers and differential aperture of the prototype stack which play a role in measuring the flux. Magnetic field is absent in this prototype. So, particles momentum can not be measured here. The results presented here provide an integrated flux of cosmic ray muons, i.e., integrated over all available energies except for those stopped in the total concrete thickness above the stack, at the sea level. A comparison of the present result with other existing measurements is also discussed at the end of the paper.

2. Cosmic ray flux distribution

The primary cosmic radiation consists of predominantly of protons, alpha particles and heavier nuclei, which interact strongly with air molecules (mainly oxygen and nitrogen nuclei) and produce mesons and other secondary particles in the collisions. Pions are one of the abundant mesons which decay to muons. Muons produced from pion decay are in the relativistic energy regime. The mean life of muons ($\sim 2.2\mu$s in its rest frame) at these energies are significantly extended due to time dilation and the muons may reach the Earth's surface before decay. Primary cosmic rays fall isotropically on top of the Earth's atmosphere. But cosmic ray flux observed on the Earth's surface (i.e., at sea level) or at a certain altitude or depth from the sea level has a zenith angular dependence. This zenith angular dependence comes from the geometrical acceptance of the detector as well as from the flux distribution itself. To investigate this cosmic muon flux distribution, a general form of the flux distribution given by $I(\theta) = I_0 cos^n\theta$ has been considered in this paper where I_0 is defined as the vertical flux and $I(\theta)$, in general, is the flux in an angle θ. Several experiments are performed globally at different places, different latitudes assuming this general form of the cosmic ray muon flux distribution and the exponent is measured. The present study is to estimate these two unknown parameters, I_0 and n, using the observed data from the prototype stack.

3. Detector set up

The prototype stack (as shown in Fig.1) used in this study consists of 12 layers of glass RPCs of 1 m $\times$ 1 m in area. The layers are labelled serially from 0 (bottom) to 11 (top). Each RPC in this cosmic ray stand has 32 strips on either side readout planes labelled as X and Y, with the strips in the X plane orthogonal to the strips in the Y plane. The width of the strips is 2.8 cm and the gap between adjacent strips is 0.2 cm. So, the strip pitch is 3 cm. The layers are stacked on top of each

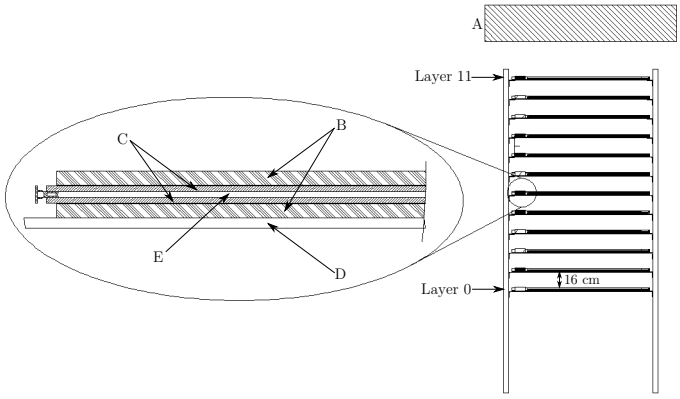

Figure 1: Elevation of the prototype stack. An RPC layer is shown with a zoomed view. A: the roof/concrete, B: Signal pick-up (HoneyComb/Polyethylene), C: Glass, D: Aluminium tray and E: RPC gas gap.

other, separated by a distance of 16 cm which amounts to a total stack height of 176 cm. Using the mechanical alignment as well as by the track fitting of cosmic ray muons, an overall hit position accuracy is obtained of about 1 mm. The RPCs are operated in avalanche mode with tracking efficiencies of 95$\pm$2% at an operating voltage of 9.9 kV. The time resolution of the chambers is about 1.5 ns. Detailed description of signal processing and Data Acquisition system (DAQ) can be found in [5] and [6]. The CAMAC DAQ mentioned in [5] has been upgraded to a VME based DAQ. Timing signals from all 32 strips from either side of electronic readout for an RPC are ORed and make a 1-fold signal. These 1-fold time signals are recorded by the TDC and these are also used to generate the cosmic ray muon trigger signal. A coincidence of these 1-fold time signals from 4 layers out of 12 layers generates the trigger. In this analysis, layer number 2, 4, 7 and 9 are used to generate the trigger. This particular choice is made in order to gain in the detector solid angular coverage. An average trigger rate of 22 Hz is observed. Total material thickness traversed by a vertical muon from the building's roof down to the second layer (as shown in Fig.1) is about 141 g cm^{-2}. Energy loss for about 1 GeV/c muon is $\sim$2 MeV per g cm^{-2} which makes minimum momentum cut off in the vertical direction about 282 MeV. Energy losses in the gas, inside the RPC or in the air, is neglected.

4. Data analysis

Strip hit information, i.e., the strip-wise hit patterns in the X and Y planes in the layers through which the particle has traversed satisfying the trigger condition, timing information and noise rate of the strips are recorded by DAQ system. Strip hit information is used for cosmic ray muon flux measurement. Noise rate of the strips is also checked to neglect any noisy strip for the entire analysis. Average hit multiplicity/cluster size is about 1.6 strips per layer for cosmic ray muon tracks. However, there are outliers (noise hits) present in the hit pattern along with actual cosmic ray muon hit, arising mainly due to correlated electronic noise [7]. In general, counting rate/noise rate per strip is observed at most to 25–30 Hz. A strip, showing high count rate ($\sim$ 100 Hz or more)

compared to others, is rejected for rest of the analysis. Either single strip hit or consecutive two or three strip hits in a layer are considered as a true cosmic ray muon signal from the RPC. The average position of these hits is finally used for track fit. Position error is assumed as $\sigma_{pos} = \frac{1}{\sqrt{12}}$ (in strip unit), i.e., about 8 mm. Event tracks due to any soft particles (limited to at most two or three layers) are neglected in this analysis and tracks which must have passed through the trigger layers are taken into consideration for this cosmic muon flux study. About 97% of events are selected out of total number of events where minimum four layer hits from X side are present for track fit and same is about 96% for Y side. About 80% of events, out of the 97% selected events for the X side, have hits from the trigger layers (layer 2, 4, 7, 9 from X side). Selected strips in X–Z and Y–Z plane are fitted separately with a straight line (Eq.4.1)

$$x/y = a \times z + b \tag{4.1}$$

where x or y are the strip/hit from the X side or Y side respectively for z-th layer, a is the slope and b is the intercept. After linear fitting, the fit point is estimated per layer along with the estimation error. A hit is rejected if the $\mid \Delta R \mid >$ one strip pitch, where ΔR is the residual defined as the difference between a hit and fit position. Another fit is made for the same event in this case with remaining hit points. It is observed after second time fit hardly ($\sim 0.001\%$) any data point is rejected. Here after first fit if any hit is rejected that is only due to outliers. But to align all detectors and to have better estimate of all tracking efficiencies this fitting process is repeated iteratively where residuals are corrected and updated in each iteration. A particular layer is excluded from fitting when its residual is estimated otherwise its residual will be underestimated. After 4/5 iterations, no appreciable change is noticed in the RMS value of the residual distributions. After last fit in last iteration results are considered for any analysis on the basis of good reduced chi-square. It is checked that X and Y side fit individually should have at least 4 layers of hits in fitting and $0 < \chi^2/ndf < 2$ is chosen for the fit results for both the sides, where ndf is the total number of points used in track fit – 2. After selecting good reconstructed muon events, it is also checked that hits must be present from the trigger layers during the track fitting and also the residual should be within one strip pitch for both the sides in these layers. This selection cut in addition to the good track reconstruction criterion together accepts about 59% of total events. The selected events, which include the trigger and tracking efficiency of the detector set up, give the proper zenith angle[1] (θ) distribution for cosmic ray muons in this prototype stack with the specified trigger criteria.

Pixel wise tracking efficiencies for all layers are estimated afterwards using fit results. A pixel is defined as 3 cm $\times$ 3 cm area in the pick-up strips as X and Y pick-up strips are orthogonal to each other. If the residual is within one strip pitch then that particular pixel is defined to be efficient. Different trigger criteria, than mentioned before, are used to get an exact pixel efficiency map for all layers so that the solid angle coverage is quite large and entire detector area can have reasonable number of events to estimate the pixel efficiency. Layers 0, 1, 3 and 4 are chosen as trigger layers to estimate pixel efficiencies for layers 6 to 11. Similarly, layers 7, 8, 10 and 11 are considered in the trigger to obtain pixel efficiencies for layers 0 to 5. The data set for these two different trigger schemes are analysed in the same way as described above in this section. Apart

[1] $\theta = cos^{-1}(\frac{h}{l})$, where h is vertical distance between the 2^{nd} and 9^{th} layer and l is the track length of a cosmic ray muon event between these two layers.

from the fitting procedure and event selection cut after track fit, as mentioned above, an additional selection criterion based upon minimising fitting error while estimating a fit point and their precise match with the hit points is used to get the pixel efficiency map. The pixel wise tracking efficiency map for the 1^{st} layer X side is shown in Fig.2. This pixel efficiency map is used in the MC analysis, discussed in the next section, to get the exact detector differential aperture including active and dead space over the RPC area.

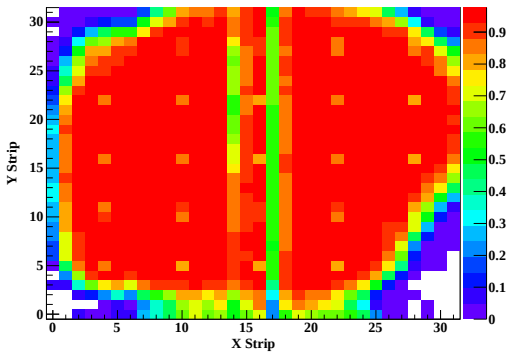

Figure 2: Tracking efficiency map for the first layer (X side).

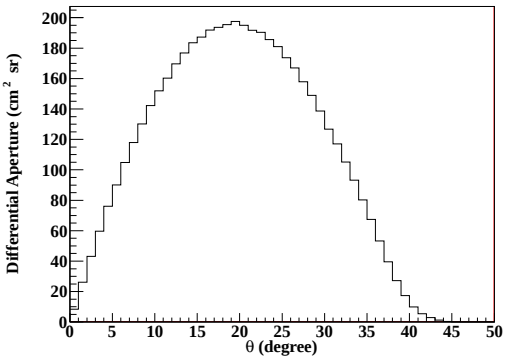

Figure 3: Differential aperture of the prototype stack.

5. Monte Carlo (MC) analysis

In the Monte Carlo process hit points in the RPC layers are simulated using uniform random numbers (between 0 to 1). A simulated event track is generated here as in the real data by first fixing a coordinate point randomly on the top trigger layer and then with respect to that point the direction is fixed by the zenith angle θ^s and azimuthal angle ϕ^s. The θ^s is generated uniformly over the solid angle and ϕ^s uniformly over the $0-2\pi$ range[1]. Different fluctuations, observed in the real data, are then included in this framework to smear hit points according to the variation in data. A hit is accepted per layer following the pixel efficiency map obtained from the data. A uniform random number is generated and if the random number is equal to or less than the efficiency of that pixel then that hit is chosen as the simulated hit. These accepted hits in various layers are then fitted to a straight line in the same way as the experimental data as discussed in Sec.4 and zenith angle distribution (θ^s) of accepted tracks is obtained. The only difference between MC and real data is that no flux effect is inherited in the simulated data. So, reconstruction of simulated tracks gives the solid angular acceptance profile of the detector set up taking into consideration all systematic effects of the detector. A proper normalisation is done to the obtained θ^s distribution, shown in Eq.5.1, to get the differential aperture (Fig. 3) for the detector set up.

$$\lambda = \frac{A\overline{N}}{N}\int_0^{\frac{5\pi}{18}} sin\theta^s d\theta^s \int_0^{2\pi} d\phi^s (\mathrm{cm}^2\mathrm{sr}) \tag{5.1}$$

[1] $X = \int msin\theta^s d\theta^s + c$, m and c are determined using the boundary condition when $X = 0, \theta^s = 0$ and for $X = 1, \theta^s = \frac{5\pi}{18}$. $Y = \int m^{'} d\phi^s + c^{'}$, where the boundary conditions are when $Y = 0, \phi^s = \pi$ and for $Y = 1, \phi^s = -\pi$. X and Y are uniform random numbers.

N is the total number of random number samples generated over the solid angle and through out the area A of the 9^{th} layer and $\overline{N}$ is the accepted number of events when points in the 2^{nd} layer are within RPC area. The θ^s is integrated up to 50° as no event is experimentally observed after that for the used trigger scheme.

6. Estimation of the parameters: I_0 and n

The experimentally observed θ distribution and the θ^s distribution for the detector solid angular acceptance are used to estimate statistically the best fit value for I_0 & n using the chi-square minimisation process. The chi-square is defined as,

$$\chi^2 = \sum_{\theta=0}^{\theta_{max}} \frac{[N^{Obs.}(\theta) - I_0 cos^n\theta \times w(\theta)]^2}{N^{Obs.}(\theta)} \tag{6.1}$$

where $N^{Obs.}(\theta)$ is experimentally observed count in a θ bin and $w(\theta)$ is the solid angular acceptance in that angle bin.

The best fit value of n (Eq.6.2) gives the actual shape for the cosmic ray muon angular distribution.

$$n = 2.150 \pm 0.011 \tag{6.2}$$

In this process, θ^s was generated uniformly over the solid angle to get the shape of the zenith angle distribution. But to estimate I_0, [1]θ^s has to be generated considering the actual cosmic ray flux distribution as obtained above. I_0 obtained afterwards from minimisation process needs a proper normalisation to give the vertical flux. The normalisation factor ξ is given by Eq.6.3.

$$\xi = \xi_{trigger} \times \xi_{selection} \times T \times \lambda^{'} \tag{6.3}$$

T is the total time (in second) taken to record the entire data set including DAQ dead time correction (about ms/event). $\xi_{trigger}$ is a fraction of selected events by the trigger condition to the number of incident events on the top trigger layer. $\xi_{selection}$ is a fraction of selected events by the track reconstruction algorithm to the number of triggered events. [2] $\lambda^{'}$ is the solid angular acceptance factor and it differs from λ as observed cosmic muon flux distribution is taken into consideration for the solid angular acceptance part. The modification for λ to $\lambda^{'}$ is necessary, otherwise ξ is overestimated and I_0 becomes underestimated. The best fit value of I_0 after normalisation comes out to be,

$$I_0 = (6.050 \pm 0.005) \times 10^{-3} \mathrm{cm}^{-2}\mathrm{s}^{-1}\mathrm{sr}^{-1} \tag{6.4}$$

The experimentally observed angular distribution of cosmic ray muon normalised by ξ is shown in Fig.4.

[1] $X = \int mcos^n\theta^s sin\theta^s d\theta^s + c$, m and c are determined using the boundary condition when $X = 0, \theta^s = 0$ and for $X = 1, \theta^s = \frac{5\pi}{18}$.

[2] $\lambda^{'} = \frac{A\overline{N}}{N} \int_0^{\frac{5\pi}{18}} cos^{2.15}\theta^s sin\theta^s d\theta^s \int_0^{2\pi} d\phi^s (\mathrm{cm}^2\mathrm{sr})$

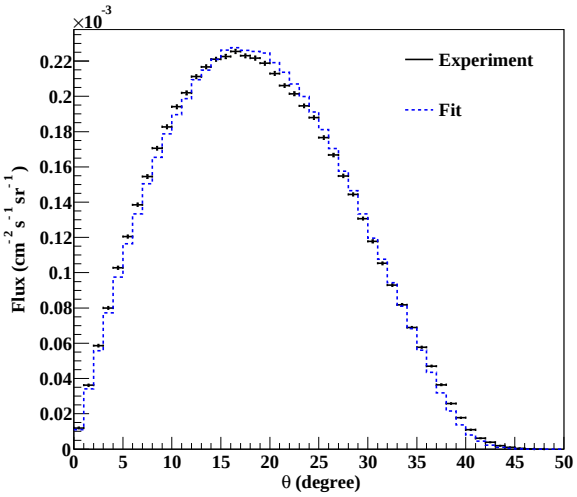

Figure 4: The normalised angular distribution of cosmic ray muons (black points with error bar) and the fitted distribution (dotted blue line)

7. Comparison with other results and discussion

A worldwide re-measurement of the muon fluxes had been initiated during 1970 to clarify the variation in the measurements. A complete set of vertical absolute integral fluxes of cosmic ray muons at or near sea level are given in Table 3.12 in [8]. A few of them are listed here in Table 1.

Table 1: Comparison of vertical integral fluxes of cosmic ray muons

Authors	Geomagnetic		Altitude (m)	Momentum (GeV/c)	Flux $\times 10^{-3}$ $(\mathrm{cm^{-2}s^{-1}sr^{-1}})$
	Lat. (°N)	[1] P_c (GV)			
Allkofer et al.[9]	9	14.1	S.L.	≥ 0.32	7.25 ± 0.1
Karmakar et al. [10]	16	15.0	122	≥ 0.353 ≥ 1.0	8.99 ± 0.05 6.85 ± 0.04
Sinha & Basu[11]	12	–	30	0.27	7.3 ± 0.2
Fukui et al.[12]	24	12.6	S.L.	≥ 0.34	7.35 ± 0.2
Present data	18	16	S.L.	≥ 0.287	6.050 ± 0.005
Rossi[13]	$\geq$50	~ 1.8	S.L.	≥ 0.32	8.3
Greisen[14]	54	1.5	S.L.	≥ 0.33	8.3 ± 0.1
Crookes & Rastin[15]	53	2.2	40	≥ 0.35	9.13 ± 0.12

Geomagnetic cut off rigidities (P_c) for cosmic rays decreases at places as going away from the equator. That is why cosmic ray muon flux is expected to increase with latitudes as moving away from the equator. Results from [13]–[15] are showing this fact. At the lower latitudes, the observed muon flux is given in [9]–[12]. The result from [10] is showing higher muon flux though the latitude and P_c are comparable with results from other lower latitudes. The present result is

[1] Geomagnetic cut off rigidities.

compared with [9], [11] and [12]; the P_c for the present site is little higher ($\sim$ 14–27%) than the other two ([9] and [12]). If only the P_c is considered then muon flux may be little less than the other two places. The lower momentum cut off is similar for all four places. The present result shows $\sim 16-17\%$ less muon flux in the vertical direction than [9] and [12].

8. Conclusion

The shape of the cosmic muon flux distribution is in agreement with existing experimental results. Cosmic muon flux measurement shows some deficit in the vertical direction as compared to existing results though detector efficiencies and other fluctuations are well considered here while estimating the differential aperture of the detector as well as the normalisation factor for the flux. This deficit could be the effect of the geomagnetic cut off rigidities for cosmic rays.

Acknowledgments

The INO project is funded by the Department of Atomic Energy (DAE) and the Department of Science and Technology (DST), Government of India. Crucial contributions from many INO collaborators to this paper are gratefully acknowledged.

References

[1] INO Collaboration, INO Project Report INO/2006/01, 2006; Detailed Project Report I,2007; Detailed Project Report on INO-ICAL Detector Structure II, 2008 (http:/www.ino.tifr.res.in/ino/OpenReports/InterimReport.pdf).

[2] V.M.Datar, et al., Nucl. Instr. and Meth. A 602 (2009) 744.

[3] M. Bhuyan, et al., Nucl. Instr. and Meth. A 661 (2012) S68-72.

[4] M. Bhuyan, et al., Nucl. Instr. and Meth. A 661 (2012) S64-67.

[5] A. Behere et al., Nucl. Instr. and Meth. A 602 (2009) p. 784.

[6] M. Bhuyan, et al., Nucl. Instr. and Meth. A661 (2012) S73-76.

[7] G.Majumder, et al., Nucl. Instr. and Meth. A 661 (2012) S77-S81.

[8] Cosmic Rays at Earth, Researcher's Reference Manual and Data Book, Peter K. F. Grieder, Elsevier, 2001.

[9] Allkofer et al., Canadian Journal of Physics, 1968, 46:(10) S301-S305, 10.1139/p68-233.

[10] N. L. Karmakar, A. Paul, and N. Chaudhuri, Nuovo Cimento B 17, 173 (1973).

[11] M. S. Sinha and N. Basu: Trans. Bose Res. Inst. (Calcutta), 21, 67 (1956-57); Indian Journ. Phys., 33, 335 (1959).

[12] S. Fukui et al., J. Phys. Soc. Japan 12, p.854 (1957).

[13] http://link.aps.org/doi/10.1103/RevModPhys.20.537, DOI:10.1103/RevModPhys.20.537.

[14] K. I. Greisen, Phys. Rev. 61, 212 (1942) & Phys. Rev. 63, 323 (1943); K. I. Greisen and N. G. Nereson, Phys. Rev. 62, 316 (1942).

[15] J. N. Crookes and B. C. Rastin, Nucl. Phys.B 39 (1972) 493-508.